

A First-Principles Equation of State of CHON for Inertial Confinement Fusion Applications

S. Zhang,¹ V. V. Karasiev,¹ N. R. Shaffer,¹ S. X. Hu,¹ D. Mihaylov,¹ K. Nichols,¹ R. Paul,¹ R. M. N. Goshadze,¹ M. Ghosh,¹ J. Hinz,¹ R. Epstein,¹ and S. Goedecker²

¹Laboratory for Laser Energetics, University of Rochester

²Department of Physics, University of Basel, Switzerland

In laser-direct-drive (LDD) inertial confinement fusion (ICF) targets, a foam layer or ablator materials with radial density gradients can mitigate laser imprint and reduce hydrodynamic instabilities during ablation.^{1,2} This can be realized by taking advantage of the two-photon polymerization (TPP) technique, which can precisely fabricate CHON polyacrylate resin into shell structures with superb lateral structure uniformity (to the level of 1 μm) (Ref. 3). To test the new ideas and optimize designs to improve target performance in relevant ICF and high-energy-density experiments, high-quality equations of state (EOS) of the target materials are required. In contrast to CH, however, which has been a widely used ablator material with relatively well understood EOS,^{4–7} an EOS for CHON is still missing.

For this study, a wide-range (0 to 1044 g/cm^3 and 0 to 10^9 K) EOS table was constructed for a C-H-O-N quaternary compound ($\text{C}_{16}\text{H}_{27}\text{O}_6\text{N}_1$, stoichiometry that matches the resin material used in the laboratory for TPP printing) from first-principles simulations. The calculations combine two state-of-the-art approaches: Kohn–Sham density functional theory molecular dynamics (KS-DFT-MD) with an accurate meta-generalized gradient approximation (GGA)-level thermal exchange-correlation functional (T-SCAN-L) and orbital-free (OF) DFT-MD with lately developed Luo–Karasiev–Trickey γ Thomas–Fermi (LKT γ TF) tunable noninteracting free-energy functionals. The thermal functional LKT γ TF is constructed through a convex combination of LKT GGA⁸ and Thomas–Fermi (TF)⁹ functionals, where γ is determined for each density by matching the pressure from our OF-DFT-MD calculations at a high temperature (1 to 3×10^5 K) to the corresponding value from the KS-DFT-MD calculations; energies from OF-DFT-MD are uniformly shifted along each isochore to align with the KS-DFT-MD values at the matching temperature. This approach is similar but superior to previous EOS studies that stitch KS and OF but use TF functional in the OF calculations.^{5,10,11} The first-principles EOS calculations are performed along 27 isochores (between 0.05 and 1044 g/cm^3) at 24 different temperatures (between 1000 and 10^9 K). The data have been extrapolated to lower densities and temperatures to produce a wide-range EOS table.

The EOS results show smooth bridging of KS and OF data at the matching condition. Figure 1 shows the EOS data approach the fully ionized ideal gas values in the limit of high temperatures (10^6 to 10^7 K, higher at higher densities). At lower temperatures, the energies and pressures for isochores of up to 4 to 7.5 g/cm^3 are below the ideal gas values because of the weaker ion and electron thermal contributions; for higher densities, the EOS increasingly exceeds the ideal gas values because of the increased degeneracy of electrons. The slope variations in the energy plots between different densities reflect changes in heat capacity; the differences between energy and pressure plots define the profile of the Grüneisen parameter. Both are caused by the joint effects of ion thermal vibration and electron thermal excitation.

Based on the calculated EOS, the predicted Hugoniot of CHON resin [Fig. 2(a)] shows a sharper profile and larger compression maximum by $\sim 2\%$ than that of pure CH polystyrene because of the coexistence of nitrogen and oxygen. Calculations of thermodynamic properties show overall consistency with that of CH along their respective Hugoniot [Figs. 2(b) and 2(c)]. Both exhibit a local minimum in heat capacity and maximum in the Grüneisen parameter at 2 to 3×10^4 K, which corresponds to

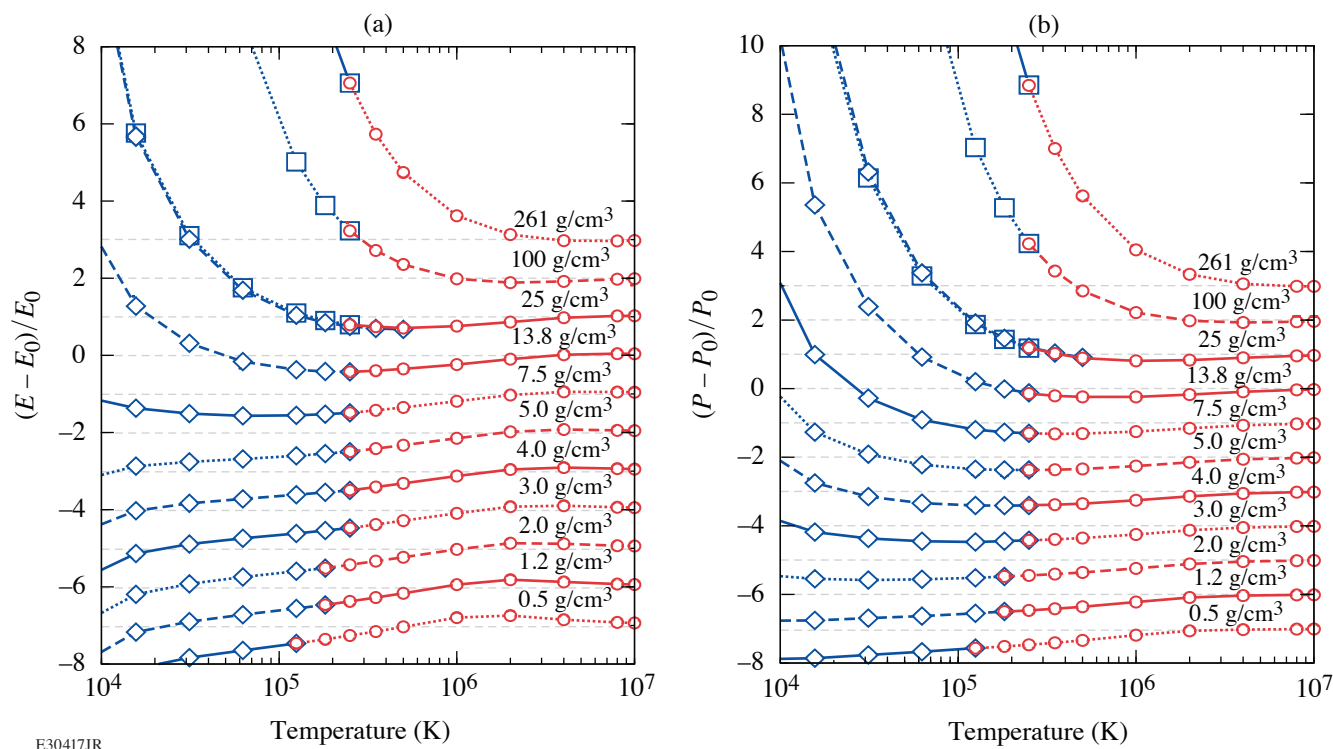


Figure 1

Matching KS (blue) and OF (red) (a) energies and (b) pressures along selected isochores. Data shown are relative to values of fully ionized ideal gas (denoted by E_0 and P_0 and shown with dashed gray horizontal lines). Blue diamonds and squares denote calculations using projector-augmented-wave and bare-coulomb potentials, respectively, which agree well with each other. Different isochores have been shifted apart for clarity.

bonded-to-atomic transition,¹² and a peak in heat capacity and a basin in the Grüneisen parameter at 10^6 K, corresponding to ionization of the K shell. The heat capacity and the Grüneisen parameters are found to reach the fully ionized ideal gas limit at 10^7 K. It is also found that the thermal expansion coefficient and the bulk sound velocity show independence of the isochore once the temperature exceeds 10^6 K.

To test the laser absorption and hydrodynamic efficiency of CHON resin as a potential ablator material for LDD targets, radiation-hydrodynamic simulations were performed of cryogenic DT implosion targets by using the 1-D radiation-hydrodynamics code *LILAC*.¹³ The CHON results are compared with the conventional CH ablator. Results from the simulations show CHON outperforms CH as the ablator for LDD target designs (Fig. 3) due to a slight increase in the laser absorption fraction, which should further prompt the fabrication of the CHON shell with a foam layer for laser-imprint mitigation.

This material is based upon work supported by the Department of Energy National Nuclear Security Administration under Award Number DE-NA0003856, the University of Rochester, and the New York State Energy Research and Development Authority. V. V. Karasiev, D. I. Mihaylov, R. M. N. Goshadze, and S. X. Hu also acknowledge support by the U.S. NSF PHY Grant No. 1802964.

1. N. Metzler, A. L. Velikovich, and J. H. Gardner, *Phys. Plasmas* **6**, 3283 (1999).
2. S. X. Hu *et al.*, *Phys. Plasmas* **25**, 082710 (2018).
3. O. Stein *et al.*, *Fusion Sci. Technol.* **73**, 153 (2018)
4. M. A. Barrios *et al.*, *Phys. Plasmas* **17**, 056307 (2010).
5. S. X. Hu *et al.*, *Phys. Rev. E* **92**, 043104 (2015).
6. S. Zhang *et al.*, *Phys. Rev. E* **96**, 013204 (2017); S. Zhang *et al.*, *J. Chem. Phys.* **148**, 102318 (2018).

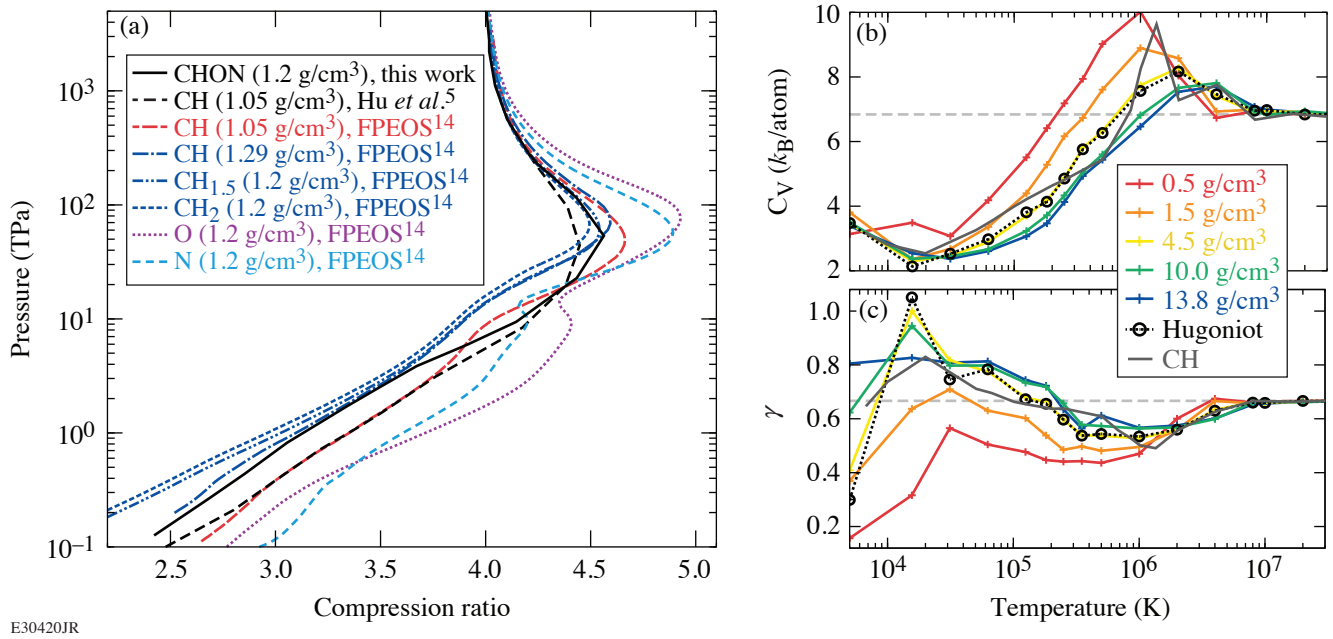


Figure 2 (a) Pressure-compression ratio Hugoniot, (b) heat capacity, and (c) Grüneisen parameter of CHON compared with that of CH. In (a), results of C–H compounds^{5,6} and of O and N from first-principles EOS¹⁴ are shown for comparison. In (b) and (c), the horizontal gray dashed lines denote the corresponding values of a fully ionized ideal gas.

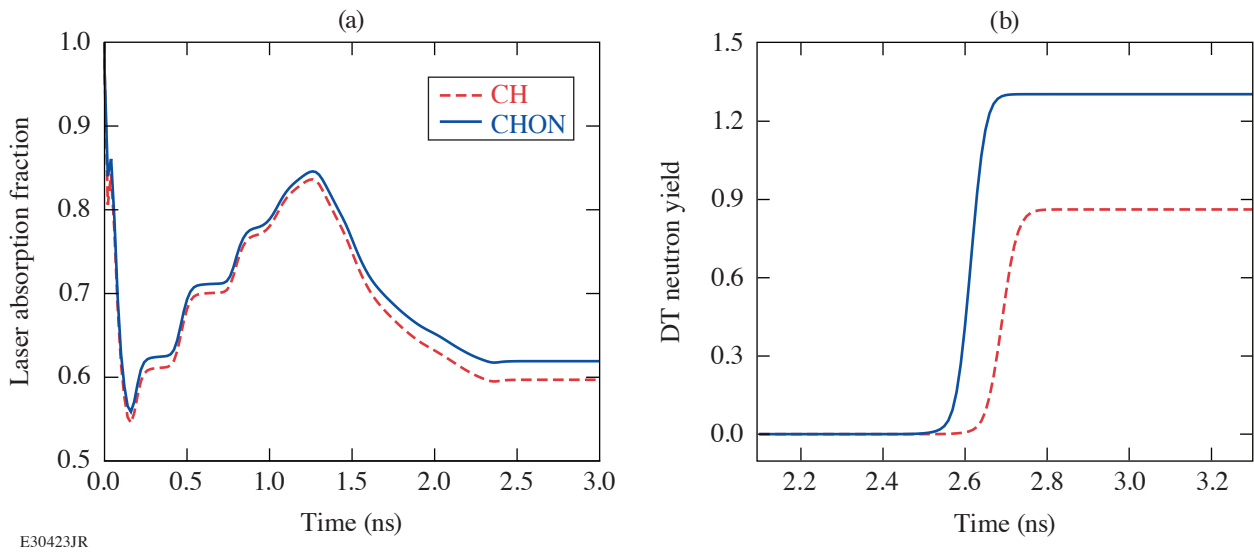


Figure 3 Comparison in (a) the time evolution of laser absorption fraction and (b) neutron yield at later time of the implosion when using targets with CH or CHON ablaters. The simulations are based on a typical OMEGA-scale cryo-DT target with a 50- μm -thick DT-ice layer covered by 8- μm -thick CH ablator ($\rho_0 = 1.05 \text{ g/cm}^3$) or 7- μm -thick CHON ablator ($\rho_0 = 1.2 \text{ g/cm}^3$) to have equivalent target mass. The simulations employ the same laser pulse (total UV laser energy of $\sim 27 \text{ kJ}$, shape optimized for the CH target assembly on OMEGA).

7. A. L. Kritcher *et al.*, *Nature* **584**, 51 (2020).
8. K. Luo, V. V. Karasiev, and S. B. Trickey, *Phys. Rev. B* **101**, 075116 (2020).
9. R. P. Feynman, N. Metropolis, and E. Teller, *Phys. Rev.* **75**, 1561 (1949).
10. S. X. Hu *et al.*, *Phys. Rev. B* **94**, 094109 (2016); *Phys. Rev. E* **95**, 043210 (2017).
11. Y. H. Ding and S. X. Hu, *Phys. Plasmas* **24**, 062702 (2017).
12. S. Zhang *et al.*, *J. Appl. Phys.* **131**, 071101 (2022).
13. J. Delettrez *et al.*, *Phys. Rev. A* **36**, 3926 (1987).
14. B. Militzer *et al.*, *Phys. Rev. E* **103**, 013203 (2021).